TWENTY-SECOND INTERNATIONAL CONFERENCE ON COMPOSITE MATERIALS (ICCM22)

ENERGY ABSORPTION MECHANISMS IN LAYER-TO-LAYER 3D WOVEN COMPOSITES

Geoffrey Neale[1], Monali Dahale[1], Sanghyun Yoo[2], Nathalie Toso[2], John Kelly[1], Cormac McGarrigle[3], Edward Archer[1], Alistair McIlhagger[1] and Eileen Harkin-Jones[1]

[1] Engineering Research Institute, Ulster University, Shore Road, Newtownabbey, BT37 0QB, UK
Email: neale-g@ulster.ac.uk, www.ulster.ac.uk/research/institutes/engineering

[2] Institute of Structures and Design, German Aerospace Centre (DLR), Stuttgart

[3]Centre for Engineering and Renewable Energy, Ulster University, Magee Campus, BT48 7JL, UK

Keywords: energy absorption, 3D composites, crashworthiness, layer-to-layer, pick density

ABSTRACT

3D woven composites provide improved out-of-plane performance over their two-dimensional counterparts. This sort of reinforced through thickness behaviour is desirable in crashworthiness applications where energy absorption can be increased by the composite material's resistance to delamination. The behaviour of these 3D materials in not well understood and fundamental data that can be used to validate and improve material models is not yet sufficiently comprehensive. Here we demonstrate that a modified layer-to-layer type 3D woven architecture can be effectively used in energy absorbing elements to produce repeatable and predictable progressive failure under axial crush conditions. Specific energy absorption (SEA) values in glass and carbon coupons of up to 62J/g and 95J/g respectively are achieved in the quasi-static regime; values up 93J/g to were achieved in the dynamic regime when carbon coupons are tested. Carbon specimens displayed uncharacteristic mixed mode failure with elements of ductile and brittle failure. The addition of a toughening agent showed mixed results in this study, providing quasi-static improvements (+8%) in SEA but significant diminishment in dynamic SEA (-22%). The failure modes present in all cases are explored in depth and the suitability of this material for industry crash applications is investigated.

1 INTRODUCTION

3D woven composites can provide sufficiently high in-plane properties, but more importantly, exceptional out-of-plane properties when compared with traditional 2D laminates [1]. These composites are fabricated from 3D woven fabric preforms which provide substantial flexibility in design, allowing for fabrics to be created with mechanical properties can be locally tailored to their intended purpose. 3D fabrics usually consist of three yarn systems which include the warp (in-plane), weft (transverse) and z-binder (through-the-thickness) yarns. These are interlaced to form a cohesive fabric at the desired thickness, negating the need for ply stacking.

At present, crashworthy 3D woven composites are not well looked into, but a few of out-of-plane impact scenarios have been investigated [2]. The main factors that hinder the progression of 3D wovens for industrial applications are: 1) the lack of a comprehensive fundamental understanding of relationships between weave variations and mechanical properties; 2) the high initial investment in loom equipment; and 3) the long time that it takes to initially set up the loom and/or change the loom setup.

Crashworthiness describes a structure's ability to absorb energy through progressive failure whilst maintaining high loads during the energy absorbing event [3]. In crashworthiness studies, reference is mostly made to a structure's energy absorption capability, which is defined by the area under the load-displacement curve, expressed in Joules (J). In composites, crashworthiness can be a function of the fibre [4], [5], matrix [6], [7], lay-up [8], [9] and interlaminar toughness properties (G_{IC}) [10]. 3D woven materials tackle the energy absorption problem by including through-thickness reinforcement, which increases the delamination resistance and damage tolerance of the composite.

Orthogonal architectures are the most extensively explored in the literature and in general show the greatest through thickness mechanical properties [11] and specific energy absorption (SEA) [12]. However, their greatest failure in this application is the high degradation of SEA with increasing and dynamic strain rates. Orthogonal architectures can lose about one third of their SEA capability when quasi-static and dynamic results are compared [13]. This contrasts with layer-to-layer architectures which show only a one sixth loss in that same comparison [13]. Layer-to-layer architectures are also able to allow for better load transfer around corners than any other established architecture [11], which is highly desirable in highly curved automotive components.

The addition of a nanofiller in composites to improve toughness is a well-established process that has been shown to be effective in increasing energy absorption. The nano-filler used in this work is calcite ($CaCO_3$) and has been selected as a cheap and readily available toughening agent. The addition of small weight percentages (1-5%) of $CaCO_3$ has been proven to increase composite toughness, flexural and compressive properties by up to 30% [14], [15]. This is generally attributed to increases in the fibre-matrix interfacial properties and increases in the matrix properties brought about by the cavitation effect. These investigations show that in percentages above 3%wt, agglomerations are more common and do not provide as efficient an effect as in lower percentages, hence the researchers in this paper have opted for a 2%wt concentration of $CaCO_3$.

This research aims to investigate the crashworthiness performance and progressive failure mechanisms in a defined iteration of 3D woven layer-to-layer composite fabricated in both glass and carbon variations. Additionally, the crush response of adding an inexpensive nanophase which has proven effective at improving toughness and compressive properties in 2D laminates is also studied. Comparisons are made amongst failure mechanisms and general behavioural differences between material sets. A further investigation into the link between the mechanical properties of the composite and its performance as a crash energy absorber is carried out.

2 MATERIALS & TESTING

2.1 3D Woven Composite

The 3D woven fabric architecture used in this study is derived from a basic layer-to-layer type architecture and is displayed in Figure 1a. The architecture consisted of three warp yarn layers (red), four weft yarn layers (white) and three binder yarns (blue) which were then interlaced to form a fabric. The addition of warp binder yarns and the way that binder layers are offset in the through the thickness direction are meant to mimic the microstructure of collagen in shells, which are able to withstand large compressive loads and crush progressively [16].

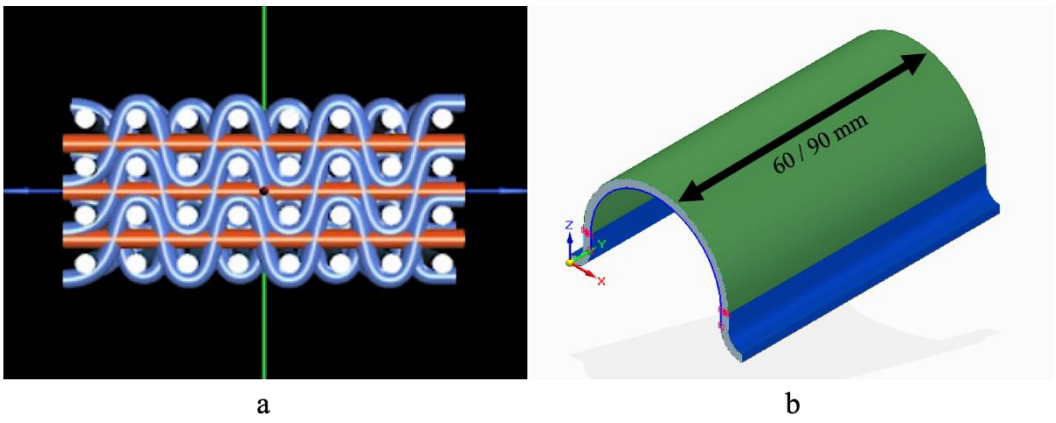

Figure 1: Diagrammatic representations of (a) layer-to-layer weave architecture (b) omega-shaped geometry

Carbon fibre preforms were manufactured from Toray T700S-50C 12k yarns and glass fibre preforms were manufactured from Hybon 2002 E-Glass (1200 Tex) yarns. Yarns were woven into 3D woven

fabric on a Jacquard loom and then infused with PRIME™ 20LV via Resin Transfer Moulding (RTM). All 3D woven fabric was designed for purpose and manufactured in-house at Ulster University with the assistance of Axis Composites Ltd. 2D carbon specimens were manufactured from XPREG XC110 Prepreg Carbon Fibre 3k, 2/2 twill with a quasi-isotropic layup [0/90, ±45/±45, 0/90]s.

For specimens toughened by the addition of the nanophase, $CaCO_3$ (calcium carbonate) nano-powder was used with an average particle size of 20nm. 2% by weight of nano-powder was added to the epoxy and mixed for 30 minutes in a high shear mixer at 1000rpm. The mixture was then placed in an ultrasonic bath for an hour. Both these processes were used to ensure an agglomerate free mixture with good dispersion.

The omega-shaped specimen geometry is based on previous work by the German Aerospace Centre (DLR) [17], [18] and is displayed in Figure 1b. The specimens consisted of a 2.5±0.5mm thick, 60±2mm (90±2mm for dynamic tests) long semi-circular section (green) with two small flanges at either end (blue). A saw tooth shaped trigger was machined into the leading edge of crush to initiate stable progressive failure. The specimens were then set into a 10mm deep resin (quasi-static) or aluminium (dynamic) base to secure during testing. This geometry was chosen for its proven stability and performance along with its ease of manufacture compared with that of closed-section 3D woven structures. Moreover, the lack of a standard for progressive crush tests and material quantity restraints require a consistent coupon with which to test the performance of these 3D woven architectures.

Table 1 shows the characteristics of the specimens used in these tests. The initial comparisons done between glass (GF-BA) and carbon (CF-BA) specimens are both manufactured with a fabric pick density of 2.5 picks/cm/layer, whereas the remaining comparisons use fabric with a pick density of 4 picks/cm/layer. Textile pick density refers to the number of weft yarns per centimetre of fabric. This change in pick density simply means that the -UN (untoughened) and -TG (toughened) specimens have 1.5 more weft yarns (yarns oriented in the 2-composite axis) per centimetre per layer than -BA specimens.

Specimen Type	Material	Pick Density (picks/cm per layer)	Mass per unit mm (g/mm)	v_f (%)	Number of Specimens
GF-BA	glass	2.5	0.381	48	4
CF-BA	carbon	2.5	0.295	40	4
CF-2D	carbon	-	0.372	55	4
CF-UN	carbon	4	0.287	40	4
CF-TG	carbon	4	0.302	40	4
CF-UN-DYN	carbon	4	0.301	40	3
CF-TG-DYN	carbon	4	0.327	40	3

Table 1: Specimen Characteristics.

2.2 Crush Testing

Quasi-static crush testing was carried out on an Instron electromechanical 5500R UTS system with 100kN load cell. Specimens were crushed at a load rate of 2mm/min for the first 15mm of displacement and the 20mm/min for the remainder of crush. The loading rate is graphically described by the red line in

Figure 5.

Dynamic crush testing was conducted on an Instron High strain VHS-100/20 with a 100kN load cell. Specimens were crushed to 60mm displacement with an initial impact speed of 8.5m/s.

Energy absorption is calculated by the area under the load-displacement plot and described mathematically by the equation:

$$E = \int F\, dx \tag{1}$$

where F is the load in kilo newtons, and x is the displacement in millimetres.

3 RESULTS & DISCUSSION

3.1 Comparison of Glass and Carbon Fibre Failure

Specimen Type	F_{max} (kN)		F_{avg} (kN)		SEA (J/g)		CFE (%)	
	Avg.	Variation (%)	Avg.	Variation (%)	Avg.	Variation (%)	Avg.	Variation (%)
GF-BA	22.8	8.1	23	5.8	61.9	5.9	101.5	3.2
CF-BA	28.8	6.9	27.6	0.9	84.2	2.5	96.4	6.3
CF-2D	34.1	3.1	30.4	5.4	84.5	2.6	88.4	4.1
CF-UN	33.3	3.3	27.5	4.3	88.5	1.4	82.5	2.2
CF-TG	33.4	1.3	29.6	2.4	94.3	1.1	88.6	1.3
CF-UN-DYN	28.6	0.0	26.6	1.9	92.9	4.6	93.0	1.9
CF-TG-DYN	26.3	7.3	24.7	5.8	75.1	6.6	93.8	1.9

Table 2: Crush results for specimens.

Table 2 and Figure 2 show the results of the crush tests on both the baseline GF-BA and CF-BA specimens. As expected, CF-BA specimens showed larger peak (F_{max}) and sustained (F_{avg}) loads, and hence a larger average SEA than GF-BA specimens, because of the superiority of carbon fibre over glass. Around a 30% difference is noted between the average recorded SEA values in GF-BA and CF-BA specimens. This percentage difference is not as pronounced as other similar experiments conducted on 2D materials reported in the literature. In a review of energy absorption mechanisms in fibre-reinforced polymers published by Carruthers et al. [19], a difference of up to 70% between these values for glass and carbon was reported amongst researchers. Researchers attribute the superiority of carbon in this application to its lower density and higher in-plane properties. Although the spread of mechanical properties amongst materials compared in that work is wide, generally the laminate layup is kept constant with only a change in the material used.

The final crush geometry for both GF-BA and CF-BA specimens are shown in Figure 4. Both carbon and glass fibre used in this study are comparable in terms of tow size, shape and "weavability." Even so, GF-BA specimens failed via splaying, which is also typical of 2D glass laminates, but CF-BA failed via a combination of progressive folding and fragmentation. In GF-BA the material splits in the middle of its cross section with the initiation of internal and external frond formation and a defined debris wedge. There is a well-defined central crush wedge with a major axial crack at the material centreline and a sequence of discontinuous circumferential transverse cracks around the specimen in fronds and are spaced apart by about the length of a yarn. In a similar quasi-isotropic distributed 2D materials, the propagation of central delamination crack during splaying is determined solely by the strength of the matrix, however energy is mostly absorbed by the bending of those fronds along with axial and transverse cracking.

In the case of this 3D material, delamination is resisted by the binding yarns which improves the effectiveness of the splaying mode in two ways. More obviously, the propagation of the central delamination crack is heavily resisted by binder yarns resulting in a very shallow debris wedge. Less obvious is the resistance of delamination between frond layers. In 2D laminates delamination would allow frond layers to slide more easily as they fold over. Here this is not the case and large circumferential cracking is introduced to allow fronds to fold over.

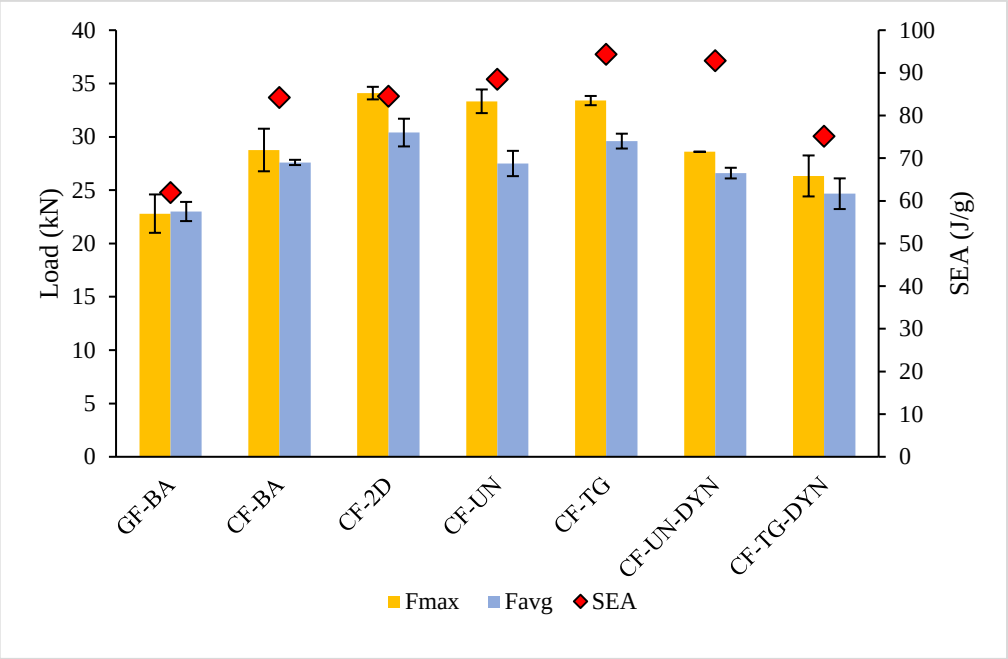

Figure 2: Crush results for all specimens tested.

The failure mechanisms observed in glass and carbon specimens here (and in the literature) are very different (Figure 4). Although the presence of z-binders completely changes the expected failure in carbon specimens (compared to 2D laminates), glass exhibits its characteristic splaying event in this 3D case. The efficiency of this failure is greatly improved compared with similar 2D aminates e.g. CF-2D, as shown by the high crush force efficiency (CFE) in GF-BA specimens. The progression of splaying as a failure mode is more so affected by the presence or improvement in through-thickness reinforcement than other progressive failure modes like brittle fracture, fragmentation and progressive folding. This is the case because splaying is actively affected by the initiation and progression of a central delamination front that causes the material to split into inward and outward fronds. When delamination is resisted in this way, large gains in SEA can be observed. This perhaps is the reason that the discrepancy between the SEA observed in carbon versus glass specimens in the literature is less pronounced than in this research.

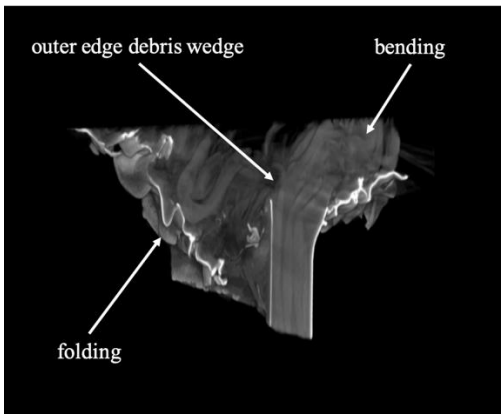

Figure 3: Micro-CT images of failure in CF-BA specimens.

An interesting observation here is the presence of some progressive folding in 3D carbon specimens (Figure 3). 2D carbon laminates would usually exhibit brittle fracture in the form of fragmentation or

splaying under this type of loading. The failure mechanisms present in CF-BA specimens are a combination of brittle fracture and progressive folding which seems to be unique to this architecture.

Brittle fracture initiated at the onset of crush with the crushing of the central yarn layers and the formation of inward and outward fronds from the external yarn layers. Post triggering, the delaminations around the central layer slip towards either the outer or inner surface edge (Figure 3). The result is usually a competing inward and outward fold at either end of the specimen (from flange to flange). The high crimp inherent in this architecture and the higher strength of carbon over glass specimens is enough to resist delamination completely under quasi-static loading. To initiate brittle fracture even some extended delamination of outer layers is required to allow the escape of crushed material in the debris wedge. Instead, the crimp induces local buckling and subsequent progressive folding.

The failure in 3D carbon specimens is in contrast with what was observed in 2D specimens (CF-2D), in which steady and controllable splaying failure developed. 3D specimens can provide similar SEA (Figure 2) as the 2D ones, with decreased peak and sustained crushing loads and a generally more efficient crush process i.e. higher CFE. Decreasing the loads experienced during crush is an important part of crashworthy design because it is this force that the occupant experiences during the crash event. In this case, the initial impact experienced by a passenger decreases by 15%. A large part of improving vehicular design is also focused on reducing the mass of components. In this test, the CF-BA specimens have a 26% lower mass per unit crush length (Table 1) than CF-2D specimens but can provide the same SEA. This works out to about 2.4J/g/mm in 3D specimens versus 2.1J/g/mm in 2D specimens.

Figure 4: Final quasi-static crush geometry in glass GF-BA (left) and carbon CF-BA (right) samples.

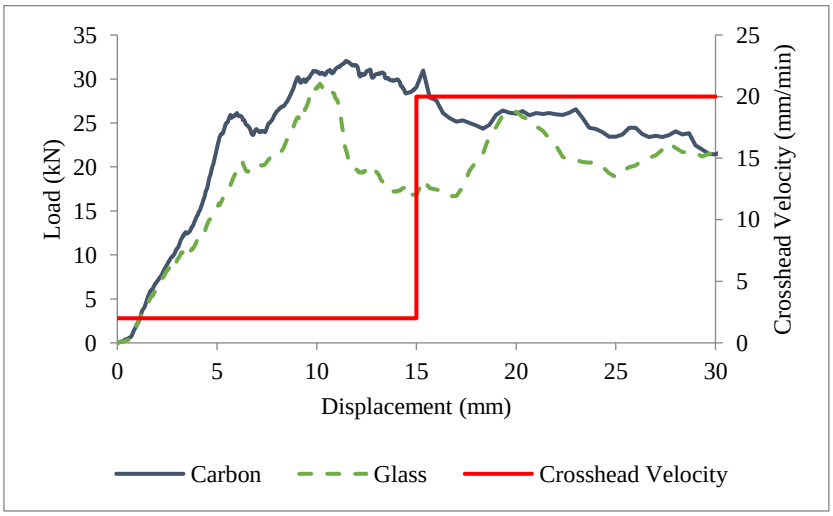

Figure 5: Typical quasi-static load versus displacement curve for glass (GF-BA) and carbon (CF-BA) specimens.

A typical load-displacement curve for GF-BA and CF-BA specimens is shown in Figure 5. The load-displacement curve in glass specimens show more regular oscillations (akin to progressive folding) than those of carbon specimens. The typical stick-slip behaviour, which is heavily pronounced in carbon curves, is somewhat combined with larger oscillatory movement of the load. The wavelength of these oscillations suggests that they correspond to the unit cell of the material (the distance over which the weave repeats itself). This supports the finding that the splaying failure in glass is resisted by the binder yarns. Each peak represents the point at which the crush front reaches a binding point and must build up stress to break the binder and proceed further.

3.2 Addition of $CaCO_3$ Nanophase

The addition of 2%wt $CaCO_3$ as a toughening agent had mixed results in this study. Table 3 shows the results of Izod impact energy tests performed on neat PRIME™ 20LV resin and on PRIME™ 20LV resin with the $CaCO_3$ nanoparticles included as a toughening agent. An 8% increase in impact energy was noted with the addition of the toughening agent.

Sample Type	No. of Specimens	Izod Impact Energy	Variation
Prime 20LV	10	1.98	14%
Prime 20LV + $CaCO_3$	10	2.12	14%

Table 3: Izod impact energy results for neat and toughened resin.

SEA was improved by 8% (Figure 2) by the addition of the $CaCO_3$ in quasi-statically tested specimens, just in line with improvements in impact energy. CF-UN specimens fail quasi-statically through pure progressive folding. Energy is primarily absorbed in flexural loading through local delaminations/debonding between yarns followed by bending resistance of the damaged material. The nanofiller acts to improve fibre-matrix interfacial adhesion and improves flexural stiffness and strength through cavitation and crack deflection resulting in a higher SEA in CF-UN specimens. Conversely, in dynamically tested specimens (CF-TG-DYN) there is a 22% decrease in SEA caused the addition of the $CaCO_3$. This suggests that the toughening mechanisms present in CF-TG specimens are ineffective in the dynamic regime.

Both specimen types fail via splaying under dynamic testing and micro-CT scans of their failure cross-sections are shown in Figure 6. CF-TG-DYN specimens display longer central delamination cracks and smaller bend radii of the created fronds than in CF-UN-DYN specimens. This suggests that the CF-TG-DYN specimens fail in a much more brittle manner than their untoughened counterparts.

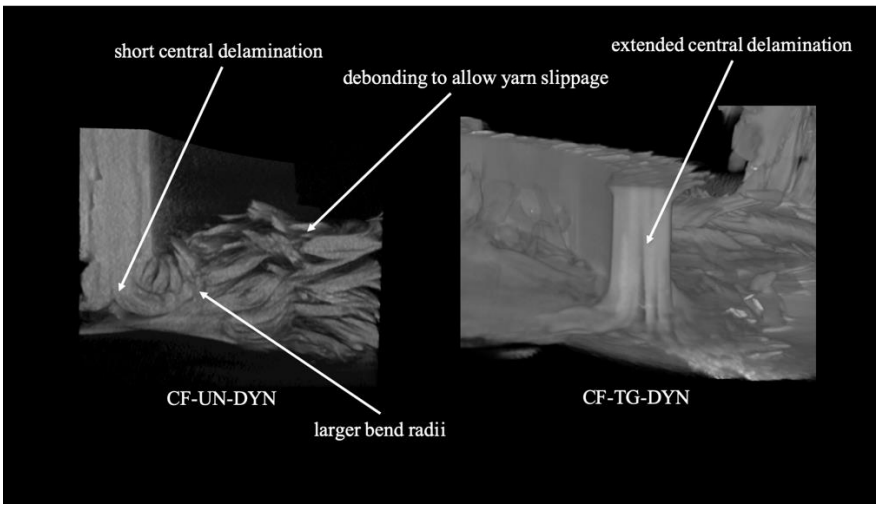

Figure 6: Micro-CT images of failure in CF-UN-DYN (left) and CF-TG-DYN (right) specimens

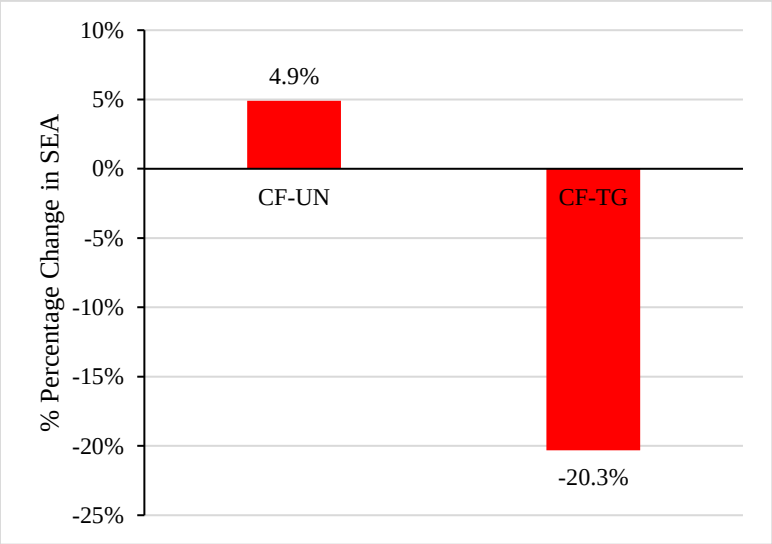

Figure 7: Percentage change in SEA in dynamic specimens as compared to quasi-static specimens.

Figure 7 shows the change in SEA in dynamic specimens as compared to their quasi-static equivalents. The untoughened specimens (CF-UN) show no decrease in SEA (in-fact showing a small increase in SEA). The same is not true for toughened specimens (CF-TG) in which a 20% decrease in SEA is noted in the transition. A significant decrease (up to 30%) between quasi-static and dynamic regimes is normal in both 2D and 3D composite materials [9], [13]. In those cases, the SEA decrease in toughened specimens usually exceeds that of untoughened ones. This phenomenon is unique to this designed fabric architecture. The final crush geometries for dynamic specimens CF-WD-DYN and CF-TG-DYN are presented in Figure 8. The crushing geometry observed in untoughened and toughened specimens describe very different failure events. In untoughened specimens, failure is via clearly defined splaying with frond formation. In toughened specimens, it appears that axial tearing on the outward fronds was more heavily restricted.

Figure 8: Final dynamic crush geometry in CF-UN-DYN (left) and CF-TG-DYN (right) specimens.

The mechanical properties of 3D woven composites are known to be strain-rate sensitive, typically increasing with increasing strain rate [2]. The specific strain rate sensitivity of the material is specific to its architecture which then determines its quasi-static compressive, tensile, flexural, shear, interlaminar properties[20], [21]. The addition of $CaCO_3$ changes the interfacial properties of the composite and helps resist delamination during failure which is evident in the hap-hazard failure geometry of the toughened specimens (Figure 8). Polymers typically embrittle with increasing strain rate allowing for an

improvement in its strength and stiffness. It is possible that as the stiffness of the polymer approaches that of the nano-filler, its effectiveness is lost and the nano-filler acts as a stress concentration rather than an energy release mechanism. Under this regime, this very brittle material would have worsened failure strains than its -UN equivalent i.e. more debonding and matrix fracture etc. (evident in the failed -TG specimens). The mechanisms by which these interfacial adhesion improvements are achieved or how the material is toughened is ineffective in the high-speed dynamic case and needs further investigation. Another possible explanation for the significant SEA reduction in CF-WD-DYN versus CF-TG-DYN is that the change in material properties brought about by the addition of $CaCO_3$ has taken the material out of the region where dynamic performance is able to outperform quasi-static performance. This phenomenon must be investigated further to be proven.

4. CONCLUSIONS

A novel 3D woven fabric architecture has been designed for providing good crush energy absorption while maintaining adequate in-plane properties. The iterations of the layer-to-layer type architecture were crushed at quasi-static loading rates of 2-20mm/min and a dynamic loading rate with an initial impact velocity of 8.5m/s. The main findings are as follows:

- Carbon specimens show a significantly higher SEA (30% higher) than glass specimens due to the increased strength and lower density of the fibres. The discrepancy between the SEA in glass and carbon specimens in this study is considerably lower than in existing published work on comparisons between glass and carbon 2D laminates. This is thought to be because the dominant splaying failure mode in glass specimens is more sensitive to the presence of binders than carbon specimens.
- Quasi-static carbon specimens were shown to exhibit a mixture of brittle fracture and progressive folding failure which is typically uncharacteristic of a brittle composite but is encouraged by the high interlacement and crimp in this 3D architecture.
- The addition of 2%wt $CaCO_3$ nanofiller was shown to provide an average 8% increase in quasi-static SEA in the material but a 22% decrease in the dynamic SEA of the material.
- Untoughened specimens show no decrease in SEA caused by a transition from quasi-static to dynamic loading whereas toughened specimens show a 20% decrease in SEA caused by the very same transition in loading. This transition is thought to result from the ineffectiveness of a stiff and brittle nano-filler in a polymer that embrittles at high strain rates.

All specimens show good quasi-static crush efficiency (on average above 80%). There was a noticeable difference in predominant failure modes and crush stability amongst specimens. A small shift in the macroscopic failure modes at play in carbon specimens was observed and characterised with the addition of the nanophase.

AKNOWLEDGEMENTS

This work was supported by EU Horizon 2020 Marie Skłodowska-Curie Actions Innovative Training Network- ICONIC [grant agreement number: 721256]. The authors acknowledge the support from The Engineering Research Centre (ECRE) of Ulster University and Axis Composites Ltd, especially Roy Brelsford, Dr Glenda Stewart, Simon Hodge and Graeme Craig.

REFERENCES

[1] A. E. Bogdanovich, “Advancements in manufacturing and applications of 3-d woven preforms and composites,” *16Th Int. Conf. Compos. Mater.*, pp. 1–10, 2006.

[2] R. Gerlach, C. R. Siviour, J. Wiegand, and N. Petrinic, “In-plane and through-thickness properties, failure modes, damage and delamination in 3D woven carbon fibre composites subjected to impact loading,” *Compos. Sci. Technol.*, vol. 72, no. 3, pp. 397–411, Feb. 2012.

[3] P. Feraboli, "Development of a Corrugated Test Specimen for Composite Materials Energy Absorption," *J. Compos. Mater.*, vol. 42, no. 3, pp. 229–256, Feb. 2008.
[4] D. W. Schmueser and L. E. Wickliffe, "Impact Energy Absorption of Continuous Fiber Composite Tubes," *J. Eng. Mater. Technol.*, vol. 109, no. 1, p. 72, 1987.
[5] P. H. Thornton, "Energy Absorption in Composite Structures," *J. Compos. Mater.*, vol. 13, no. 3, pp. 247–262, Jul. 1979.
[6] N. A. Warrior, T. A. Turner, F. Robitaille, and C. D. Rudd, "Effect of resin properties and processing parameters on crash energy absorbing composite structures made by RTM," *Compos. Part A Appl. Sci. Manuf.*, vol. 34, no. 6, pp. 543–550, Jun. 2003.
[7] T. A. Turner, F. Robitaille, N. A. Warrior, C. D. Rudd, and E. J. Cooper, "Effect of resin formulation on crash energy absorbing composite structures made by RTM," *Plast. Rubber Compos.*, vol. 31, no. 2, pp. 49–57, Feb. 2002.
[8] S. Ramkrishna, H. Hamada, and Z. Maekawa, "Energy Absorption Behavior of Carbon-Fiber-Reinforced Thermosplastic Composite Tubes," *J. Thermoplast. Compos. Mater.*, vol. 8, no. 3, pp. 323–344, Jul. 1995.
[9] A. Jackson, S. Dutton, A. J. Gunnion, and D. Kelly, "Investigation into laminate design of open carbon-fibre/epoxy sections by quasi-static and dynamic crushing," *Compos. Struct.*, vol. 93, no. 10, pp. 2646–2654, 2011.
[10] D. T. Fishpool, A. Rezai, D. Baker, S. L. Ogin, and P. A. Smith, "Interlaminar toughness characterisation of 3D woven carbon fibre composites," *Plast. Rubber Compos.*, vol. 42, no. 3, pp. 108–114, Apr. 2013.
[11] M. N. Saleh and C. Soutis, "Recent advancements in mechanical characterisation of 3D woven composites," *Mech. Adv. Mater. Mod. Process.*, vol. 3, no. 1, p. 12, Dec. 2017.
[12] H. Bayraktar *et al.*, "3D Woven Composites for Energy Absorbing," in *20th International Conference on Composite Materials*, 2015, no. July, pp. 19–24.
[13] J. Goering and H. Bayraktar, "3D Woven Composites for Energy Absorption Applications," in *SPE automotive*, 2016, no. April, pp. 1–18.
[14] A. Abdi, R. Eslami-Farsani, and H. Khosravi, "Evaluating the Mechanical Behavior of Basalt Fibers/Epoxy Composites Containing Surface-modified CaCO3 Nanoparticles," *Fibers Polym.*, vol. 19, no. 3, pp. 635–640, Mar. 2018.
[15] V. Eskizeybek, H. Ulus, H. B. Kaybal, Ö. S. Şahin, and A. Avcı, "Static and dynamic mechanical responses of CaCO3 nanoparticle modified epoxy/carbon fiber nanocomposites," *Compos. Part B Eng.*, vol. 140, no. July 2017, pp. 223–231, 2018.
[16] P. Fratzl and R. Weinkamer, "Nature's hierarchical materials," *Prog. Mater. Sci.*, vol. 52, no. 8, pp. 1263–1334, Nov. 2007.
[17] D. Kohlgrueber and A. Kamoulakos, "Validation of Numerical Simulation of Composite Helicopter Sub-floor Structures under Crash Loading," in *American Helicopter Society 54th Annual Forum*, 1998.
[18] M. David, A. F. Johnson, and H. Voggenreiter, "Analysis of Crushing Response of Composite Crashworthy Structures," *Appl. Compos. Mater.*, vol. 20, no. 5, pp. 773–787, Oct. 2013.
[19] J. J. Carruthers, A. P. Kettle, and A. M. Robinson, "Energy Absorption Capability and Crashworthiness of Composite Material Structures: A Review," *Appl. Mech. Rev.*, vol. 51, no. 10, p. 635, 1998.
[20] J. Zhao, L. Zhang, L. Guo, and Y. Yang, "Dynamic properties and strain rate effect of 3D angle-interlock carbon/epoxy woven composites," *J. Reinf. Plast. Compos.*, vol. 36, no. 20, pp. 1531–1541, 2017.
[21] B. Sun and B. Gu, "Shear behavior of 3D orthogonal woven fabric composites under high strain rates," *J. Reinf. Plast. Compos.*, vol. 25, no. 17, pp. 1833–1845, 2006.